Title

The formation of cortical actin arrays in human trabecular meshwork cells in response to cytoskeletal disruption

Journal

Experimental Cell Research, 328(1)

ISSN

0014-4827

Authors

Murphy, Kaitlin C
Morgan, Joshua T
Wood, Joshua A
et al.

Publication Date

2014-10-01

DOI

10.1016/j.yexcr.2014.06.014

Peer reviewed

Published in final edited form as:
Exp Cell Res. 2014 October 15; 328(1): 164–171. doi:10.1016/j.yexcr.2014.06.014.

The Formation of Cortical Actin Arrays in Human Trabecular Meshwork Cells in Response to Cytoskeletal Disruption

Kaitlin C. Murphy[#1], **Joshua T. Morgan**[#2], **Joshua A. Wood**[2], **Adeline Sadeli**[2], **Christopher J. Murphy**[2,4], and **Paul Russell**[2,*]

[1]Department of Biomedical Engineering / University of California, Davis

[2]Department of Surgical and Radiological Sciences, School of Veterinary Medicine / University of California, Davis

[4]Department of Ophthalmology & Vision Science, School of Medicine / University of California, Davis

[#] These authors contributed equally to this work.

Abstract

The cytoskeleton of human trabecular meshwork (HTM) cells is known to be altered in glaucoma and has been hypothesized to reduce outflow facility through contracting the HTM tissue. Latrunculin B (Lat-B) and Rho-associated protein kinase (ROCK) inhibitors disrupt the actin cytoskeleton and are in clinical trials as glaucoma therapeutics. We have previously reported a transient increase in HTM cell stiffness peaking at 90 minutes after Lat-B treatment with a return to pretreatment values after 270 minutes. We hypothesize that changes in actin morphology correlate with alterations in cell stiffness induced by Lat-B but this is not a general consequence of other cytoskeletal disrupting agents such as Rho kinase inhibitors. We treated HTM cells with 2 μM Lat-B or 100 μM Y-27632 and allowed the cells to recover for 30-270 min. While examining actin morphology in Lat-B treated cells, we observed striking cortical actin arrays (CAAs). The percentage of CAA positive cells (CPCs) was time dependent and exceeded 30% at 90 minutes and decreased after 270 minutes. Y-27632 treated cells exhibited few CAAs and no changes in cell stiffness. Together, these data suggest that the increase in cell stiffness after Lat-B treatment is correlated with CAAs.

Keywords

Trabecular Meshwork; Cytoskeleton; Actin; Rho-associated protein kinase

[*]Corresponding Author: Department of Surgical and Radiological Science School of Veterinary Medicine 1 Shields Ave. University of California Davis, CA 95616 Phone: (530) 752-3676 prussell@ucdavis.edu.

1. Introduction

Glaucoma is a leading cause of irreversible blindness worldwide and is predicted to impact 79.6 million people by 2020 [1]. Primary open angle glaucoma (POAG) is the most common form of glaucoma and in the majority of cases is associated with elevated intraocular pressure (IOP) [2]. Increased resistance to outflow of aqueous humor through the human trabecular meshwork (HTM) into Schlemm's canal is thought to be a major contributor to elevated IOP [3-5]. For that reason, the cells that populate the HTM are believed to be important to the regulation of the outflow of aqueous humor and the development of elevated IOP and glaucoma [4, 6].

Decreasing IOP is currently the only medically recognized method for the treatment of POAG, but none of the commercially available glaucoma medications specifically target outflow through the HTM cells [7-10]. Filamentous actin (F-actin) of the HTM is known to play a role in aqueous flow dynamics and it has been speculated that the organization and contractility of the actin cytoskeleton increases the stiffness of HTM cells and hinders the outflow of aqueous humor, thereby increasing IOP [11, 12]. It is possible this plays a role in overall stiffness of HTM tissue, which we have recently shown is greater than 20 fold stiffer in glaucoma [13].

Bolstering the casual linkage between outflow and HTM cytoskeleton regulation, compounds that increase or decrease contractility also influence outflow resistance. For example, compounds thought to increase contractility of the actin cytoskeleton such as dexamethasone [11] and lysophospholipids [14-17] are known to reduce outflow facility. Cytoskeletal associated proteins have also been investigated in this regard. Cochlin, a putative mechanosensor, is upregulated in glaucoma, increases outflow resistance, and has been linked to altered actin morphology in HTM cells [18-21]. AMP-activated protein kinase (AMPK) signaling increases outflow with a mechanism that includes decreased F-actin and stress fiber formation [22]. Delivery of exogenous platelet-derived growth factor or profilin I, both actin regulators, likewise increases outflow in cultured anterior segments [23, 24]. These examples underline the importance of the cytoskeleton in outflow regulation, leading to considerable interest in pharmacologically disrupting HTM cytoskeleton as a potential glaucoma therapeutic.

Examples of potential cytoskeleton-targeting therapeutics are Latrunculin B (Lat B) and Rho-associated protein kinase (ROCK) inhibitors [25]. Both have been shown to increase outflow facility [26-29]. Lat B reversibly inhibits actin polymerization resulting in disruption of the actin cytoskeleton [30]. The mechanism of action of ROCK inhibitors, such as Y-27632, is different. ROCK is a potent stabilizer of the actin cytoskeleton and activator of contractility. Inhibitors such as Y-27632 reduce cellular contractility and the stability of actin fibers, resulting in fewer stress fibers but not complete ablation of the actin cytoskeleton [31]. We have recently shown that Lat B treatment dramatically softens HTM cells as expected with the ablation of the actin cytoskeleton. However, after Lat B removal there is a significant and transient increase in HTM cell stiffness [32]. The following studies were undertaken to determine the morphology of the actin cytoskeleton during the transient stiffening as it recovers after Lat B treatment. We examined the effects of Y-27632 to see if

increases in stiffness and actin organization during recovery were general phenomena of actin reassembly after disruption.

2. Methods

2.1 Cell Culture, Cytoskeletal Treatments

Primary HTM cells were isolated from donor corneoscleral rims (Saving Sight Eye Bank, St. Louis, MO) as described previously [33]. All experiments were performed in compliance with the Declaration of Helsinki. HTM cells were cultured in DME/F 12,1:1 medium (Fisher Scientific, Waltham, MA) with 10% fetal bovine serum (Atlanta Biologicals, Lawrenceville, GA) and 2 mM penicillin, streptomycin, amphotericin-B (Lonza, Basel, Switzerland). The HTM cells were seeded on 12-well tissue culture plastic (TCP) plates at a low density of 30,000 cells per well and allowed to attach for 24 hours. The cells were then placed in Dulbecco's phosphate buffered saline (DPBS; Hyclone, Logan, UT) supplemented with either Lat B or Y-27632 as described below.

For Lat B experiments, the cells were treated with either a 2 μM solution of Latrunculin-B (Lat B) (Cal Biochem, La Jolla, CA) dissolved in dimethyl sulfoxide (DMSO) (Fisher Scientific, Waltham, MA) or DMSO as a vehicle control for 30 minutes, after which the treatment solution was removed and the cells were placed in culture medium where they were allowed to recover for 0, 30, 50, 90, or 270 minutes.

For Y-27632 experiments, cells were treated with either a 100 μM solution of Y-27632 (Sigma, St. Louis, MO) dissolved in water (Hyclone, Logan, UT) or water as a vehicle control. As above, the treatments lasted for 30 minutes, after which the cells were allowed to recover in full medium for 30 or 90 minutes.

2.2 Fluorescent Labeling of Actin Structures

In order to visualize the F-actin, cells were fixed for 60 minutes in 1% gluteraldehyde (Poly Scientific, Bay Shore, NY) and 0.5% Triton-X 100 (Fisher Scientific, Waltham, MA) in PBS and later stained with Alexa-Flour 568 Phalloidin (Invitrogen, Carlsbad, CA).

For improved α-actinin visualization, cells were fixed in -20º C methanol for 20 minutes and air-dried. The cells were than co-stained with mouse anti-α-actinin (clone AT6/172, Millipore, Temecula, CA) and rabbit anti-actin (Sigma, St. Louis, MO) followed by Alexa-Flour 488 labeled goat anti-mouse IgG and Alexa-Flour 594 labeled goat anti-rabbit IgG (Invitrogen, Carlsbad, CA).

2.3 Imaging and Image Analysis

The HTM cells were imaged using an inverted fluorescent microscope (Zeiss, Axiovert 200M) at 20X magnification. Within each well a 32 square mm area was imaged by combining 225 images (450 μm x 335 μm / image). Of the cells found in this area, only the cells that were not in contact with another cell were analyzed resulting in approximately 100-200 cells being analyzed per experimental condition. These cells were counted in a binary fashion as either cortical actin arrays (CAA) positive or CAA negative. A cell was considered CAA positive if it had multiple circumferentially oriented actin filaments along

the entire cell periphery (Fig. 1B). The results for each given condition are expressed as percent of CAA positive cells.

2.4 Measurement of Cell Mechanics

Cell mechanics were determined as described previously using the Asylum MFP-3D-Bio atomic force microscope (AFM) [32]. Briefly, prior to each experiment the AFM probes were exposed to UV (UV/Ozone Procleaner, BioForce Nanoscience, Ames, IA) for 1 hour to effectively remove organic contaminants. After equilibrating the samples in 1X DPBS, the samples were indented by using contact mode with silicon nitride cantilevers (PNP-TR-50, length = 100 μm, actual k = 44 - 231 pN/nm, Nano World, Switzerland) with square pyramidal tips. Each cantilever was calibrated to obtain the actual spring constant which varied from the manufacturer's nominal value. The actual spring constant was determined by performing thermal tune to measure the cantilever's response to thermal noise. The deflection sensitivity was obtained by taking the average of 5 force curves on a glass slide in DPBS.

The elastic modulus (E) of each sample was obtained by fitting indentation force versus indentation depth of the sample with the overlay of the theoretical force based on Hertz model as shown in Eq. 1 for rigid pyramidal tip geometry.

$$F = \frac{2}{\pi} \frac{E \tan(\alpha)}{1 - v^2} \delta^2 \quad (1)$$

Where F is the force applied by indenter, α is the tip half angle (35°), ν is Poisson's ratio (assumed to be 0.5), and δ is indentation depth. The Hertz model assumes that the samples were linearly elastic, homogenous, and infinitely thick. However, in the limit of small deformations, the Hertz model can be used for materials (such as cells) which are viscoelastic, heterogeneous, and finite [34].

For consistency, cells were only selected for measurement if they were not in contact with other cells. They were compressed five times at 2 μm/s with the contact point centered above the cell nucleus, to minimize variability due to cell geometry. Contact point was detected where the cantilever's deflection deviated from the zeroed deflection. Young's modulus was determined from the plot of force versus indentation. To ensure representative data, five cells were measured for each treatment condition and the experiment was repeated with cells isolated from five donors. Measurements were performed in DPBS (Hyclone, Logan, UT). Cells were treated with 100 μM Y-27632 for 30 minutes as described above and then allowed to recover in media for either 90 or 270 minutes before measurement.

2.5 Statistics

All experiments were replicated with cells isolated from multiple donors (three for CAA characterization and counting; and five for cell mechanics measurements). No differences were observed among donors and the resulting data were pooled. Data were analyzed using the SigmaPlot 11 (Systat, Chicago, IL) software package. One-way ANOVA was used to determine significance followed by Tukey's post-hoc for pairwise comparisons.

Significances between values in comparison to the pre-treatment value are denoted with '*', and significances between the Lat B value and its corresponding DMSO control value at the same time point are denoted with '#'. All levels of significance are defined as ***/### = $p<0.001$ and **/## = $p<0.01$. All data are presented as mean ± SEM.

3 Results

3.1 Observation of CAAs in HTM cells

In both isolated and confluent HTM cells, phalloidin staining revealed prominent axial stress fibers in the majority of cells (Fig. 1A). Additionally, cortical actin arrays (CAAs), comprised of parallel circumferential actin fibers regularly intersected by radial cross linking fibers, were observed in ~3% of cells (Fig. 1B). In order to determine if the intersections were sites of cross-linking between the cortical and radial filaments, we stained for α-actinin, previously associated with cross-linking in other higher order actin structures [35-38]. The α-actinin stain revealed heavy labeling at the junctions (arrow heads, Fig. 1C) and along the radial filaments, consistent with the concept of cross-linking between the radial and cortical actin. The staining also revealed periodic α-actinin staining along the circumferential actin bundles, reminiscent of stress fibers [39-41] (bracket, Fig. 1C). While examining cells for the presence of CAAs it was noted that there were distinct variations of these structures within the HTM cells which could be subcategorized as ringed, clustered, or angular (Fig. 1D).

3.2 CAA formation after Latrunculin B treatment

To observe the effect of disrupting the actin cytoskeleton on the incidence of CAAs, we treated cells with 2 μM Lat B for 30 minutes. This dose was sufficient to completely remove any F-actin staining (Fig. 2A). HTM cells were then allowed to recover in serum containing media. The cells contained CAAs in differing proportions throughout their recovery time (Fig. 2B), while untreated or DMSO treated cells exhibited few (~3%) CAAs, regardless of time point. Immediately after Lat B treatment (0 minutes), there was complete disruption of F-actin and no actin structures (including CAAs) were observed. Remarkably, CAAs were formed in non-confluent cells within as little as 30 minutes of recovery. The percent of CAA positive cells steadily increased until 90 minutes, where it peaked at 32.5±2.1% (mean ±SEM, n=9). At 270 minutes, the percentage of CAAs was approaching that found pretreatment, although still significantly elevated.

While reviewing the entire 32 mm^2 area it was observed that the CAA positive cells were usually located in close proximity to each other (Fig. S1A), and were rarely observed isolated from other CAA positive cells. Additionally, small circular bundles of actin remained in the peri-nuclear region and in the cytoplasm at the end of the Lat B treatment and they persisted throughout the recovery period (arrowheads, Fig. S1B). This may be due to the residual Lat B present in the cells as a result of the short recovery time used in this study. These bundles were not observed in HTM cells treated with DMSO.

3.3 ROCK inhibition with Y-27632

Treatment of HTM cells with 100 μM Y-27632 for 30 minutes was sufficient to disrupt stress fibers of the actin cytoskeleton (Fig. 3A). The cells were then allowed to recover for 30 or 90 minutes, corresponding to previously reported key time points in the Lat B response, and assayed for CAA induction. At these timepoints, cells typically had not yet returned to their elongated morphologies, but did exhibit aligned stress fibers (Fig. 3B). CAAs were not induced by Y-27632 at either time point (Fig. 3C; $p<0.7346$).

To determine if cell stiffness was altered during recovery from ROCK inhibition, we treated cells with 100 μM Y-27632 for 30 minutes and allowed them to recover for 90 and 270 minutes, consistent with the timepoints of the previously reported Lat B study [32]. We found no changes in cell stiffness at either time point (Fig. 3D; $p = 0.6924$). As the effect of Y-27632 appeared to be more transient than Lat B, with stress fibers reforming at 30 and 90 min (Fig. 3B), we next considered the possibility that CAAs formed at earlier timepoints. To test this, we assayed for CAA induction at 0, 10, 15, 20, and 25 minutes after Y-27632 washout. At 15 minutes, actin filaments became visible in some cells (Fig. 4A). No significant induction of CAAs occurred at these timepoints (Fig. 4B).

4. Discussion

In this work, we describe cross-linked cortical actin structures exhibited by HTM cells (Fig. 1B-D) and their induction by Lat B (Fig. 2), but not Y-27632 treatment (Figs. 3 and 4). These were transient structures, with induction occurring from 30-90 minutes and their incidence declining by 270 minutes. These structures were constructed of a band of cortical actin filaments exhibiting α-actinin staining patterns typical of contractile actin, cross-linked by heavily α-actinin labeled radial fibers. In our analysis we employed a very stringent definition for considering a cell CAA positive: requiring the CAA to completely encircle the nucleus and the cell to be isolated from other cells. Using less stringent definitions would have substantially increased the percentage of CAA positive cells, but would have also introduced a more subjective threshold for inclusion (such as the number of junctions, area covered, etc.) which we wished to avoid.

It is instructive to compare these results to other higher order actin cytoskeletal structures of HTM cells. Cross-Linked Actin Networks (CLANs) are polygonal structures that are formed by α-actinin enriched junctions between actin filaments [11, 35-38, 42-47]. Initial work characterizing CLANs identified them as transient structures appearing shortly after plating, and suggested that they are precursors to stress fibers [37, 38] and sarcomeres [47]. In the majority of previous reports, CLANs in HTM cells were induced after extended (4-14 day) incubations with dexamethasone [11, 35, 42, 43], although CLANs have recently been reported as early as a few hours after plating by activating integrin signaling pathways with [35] or without [36, 44] extended dexamethasone treatment. CAAs, as detailed above, are α-actinin enriched actin networks that form in as little as 30 minutes following Lat B washout and disappear after a few hours. While also an α-actinin enriched actin network, CAAs are substantially more transient structures that span the entire cell, demonstrating they are distinct from traditional CLANs.

We specifically matched the experimental conditions to our previous work describing the mechanics of HTM cells after Lat B treatment [32] such that we could compare the actin geometry and cell mechanics after Lat B treatment. Treatment with Lat B resulted in a transient increase in stiffness 90 minutes after washout, which was gone by 270 minutes [32]. Importantly, CAAs were strongly induced by 90 minutes (32.48 ± 6.29%) and which declined to 11.03 ± 5.18% at 270 minutes (Fig. 2B). The correlation of increased cell stiffness with CAA formation suggests these phenomena may be promoted by a shared mechanism or are causally linked. Additionally, the circumferential actin bundles were decorated with periodic α-actinin labeling (Fig. 1C), a characteristic shared with contractile actin structures [39-41] in other cell lines. This suggests that these structures are contractile in nature, which could result in increased stiffness. It is important to note that the comparison between the increase in CAA presence and cell stiffness during Lat B recovery involves analysis of populations of cells without specific knowledge of the cytoskeletal geometry of the individual cells. At this time, the data points to the presence of CAAs and cellular stiffening as epiphenomena, two features of actin reassembly following Lat B treatment. Additional studies would be needed to measure both mechanics and CAAs or other cytoskeletal structures within the same cell to rigorously correlate the two behaviors.

The mechanism for the observed CAA formation following recovery from Lat B treatment is unknown. CAA positive cells tended to appear in groups, suggesting that CAA formation is influenced by differences in local matrix composition or paracrine signaling. These concepts are in line with previous work identifying glucocorticoids [11, 35, 42, 43] and integrin (β1 and β3) [35, 36, 44] signaling as mediators of CLAN formation. It is possible the CAAs we described are mediated by similar pathways.

Finally, we demonstrated that the induction of CAAs and cell stiffening is not generalizable to the action of actin cytoskeletal disrupting agents. To this end, we employed the ROCK inhibitor Y-27632, which destabilizes stress fibers and decreases contractility [31]. While ROCK inhibition did ablate stress fibers and cause dramatic changes to cell morphology, after washout the cells quickly recovered stress fibers (Fig. 3A) in contrast to Lat B treated cells (Fig. 2A). Additionally, Y-27632 did not induce CAA formation or stiffening upon recovery (Figs. 3 and 4). This has important implications for the use of cytoskeletal disruptors in glaucoma therapy. Glaucomatous HTM exhibits both altered actin geometries [11] and elevated stiffness [13]. Both of these properties were exhibited *in vitro* by HTM cells during recovery from Lat B but not Y-27632. *In vivo*, it is not known if these changes occur with Lat B treatment since published results have timeframes post treatment when it might be anticipated that the short term stiffening would no longer be observed. Further studies are needed to elucidate the *in vivo* relationship between CAA formation and cell stiffening in HTM cells.

Supplementary Material

Refer to Web version on PubMed Central for supplementary material.

Acknowledgments

This work was funded by grants from the National Institutes of Health R01EY019475, R01EY019970 and P30EY12576, a grant from National Glaucoma Research, a program of the American Health Assistance Foundation and an unrestricted grant from Research to Prevent Blindness.

References

[1]. Quigley HA, Broman AT. The number of people with glaucoma worldwide in 2010 and 2020. Br J Ophthalmol. 2006; 90:262–267. [PubMed: 16488940]

[2]. Quigley HA. Open-angle glaucoma. N Engl J Med. 1993; 328:1097–1106. [PubMed: 8455668]

[3]. Johnstone MA, Grant WG. Pressure-dependent changes in structures of the aqueous outflow system of human and monkey eyes. Am J Ophthalmol. 1973; 75:365–383. [PubMed: 4633234]

[4]. Johnson M. 'What controls aqueous humour outflow resistance?'. Exp Eye Res. 2006; 82:545–557. [PubMed: 16386733]

[5]. Maepea O, Bill A. Pressures in the juxtacanalicular tissue and Schlemm's canal in monkeys. Exp Eye Res. 1992; 54:879–883. [PubMed: 1521580]

[6]. Goel M, Picciani RG, Lee RK, Bhattacharya SK. Aqueous humor dynamics: a review. The open ophthalmology journal. 2010; 4:52–59. [PubMed: 21293732]

[7]. Zhang K, Zhang L, Weinreb RN. Ophthalmic drug discovery: novel targets and mechanisms for retinal diseases and glaucoma. Nat Rev Drug Discov. 2012; 11:541–559. [PubMed: 22699774]

[8]. Heijl A, Leske MC, Bengtsson B, Hyman L, Hussein M. Reduction of intraocular pressure and glaucoma progression: results from the Early Manifest Glaucoma Trial. Arch Ophthalmol. 2002; 120:1268–1279. [PubMed: 12365904]

[9]. Heijl A, Leske MC, Hyman L, Yang Z, Bengtsson B. Intraocular pressure reduction with a fixed treatment protocol in the Early Manifest Glaucoma Trial. Acta Ophthalmol. 2011; 89:749–754. [PubMed: 20236252]

[10]. Comparison of glaucomatous progression between untreated patients with normal-tension glaucoma and patients with therapeutically reduced intraocular pressures. Collaborative Normal-Tension Glaucoma Study Group. Am J Ophthalmol. 1998; 126:487–497. [PubMed: 9780093]

[11]. Clark AF, Brotchie D, Read AT, Hellberg P, English-Wright S, Pang IH, Ethier CR, Grierson I. Dexamethasone alters F-actin architecture and promotes cross-linked actin network formation in human trabecular meshwork tissue. Cell Motil Cytoskeleton. 2005; 60:83–95. [PubMed: 15593281]

[12]. Tian B, Geiger B, Epstein DL, Kaufman PL. Cytoskeletal involvement in the regulation of aqueous humor outflow. Invest Ophthalmol Vis Sci. 2000; 41:619–623. [PubMed: 10711672]

[13]. Last JA, Pan T, Ding Y, Reilly CM, Keller K, Acott TS, Fautsch MP, Murphy CJ, Russell P. Elastic modulus determination of normal and glaucomatous human trabecular meshwork. Invest Ophthalmol Vis Sci. 2011; 52:2147–2152. [PubMed: 21220561]

[14]. Mettu PS, Deng PF, Misra UK, Gawdi G, Epstein DL, Rao PV. Role of lysophospholipid growth factors in the modulation of aqueous humor outflow facility. Invest Ophthalmol Vis Sci. 2004; 45:2263–2271. [PubMed: 15223804]

[15]. Boussommier-Calleja A, Bertrand J, Woodward DF, Ethier CR, Stamer WD, Overby DR. Pharmacologic manipulation of conventional outflow facility in ex vivo mouse eyes. Invest Ophthalmol Vis Sci. 2012; 53:5838–5845. [PubMed: 22807298]

[16]. Sumida GM, Stamer WD. S1P(2) receptor regulation of sphingosine-1-phosphate effects on conventional outflow physiology. Am J Physiol Cell Physiol. 2011; 300:C1164–1171. [PubMed: 21289286]

[17]. Stamer WD, Read AT, Sumida GM, Ethier CR. Sphingosine-1-phosphate effects on the inner wall of Schlemm's canal and outflow facility in perfused human eyes. Exp Eye Res. 2009; 89:980–988. [PubMed: 19715693]

[18]. Goel M, Sienkiewicz AE, Picciani R, Lee RK, Bhattacharya SK. Cochlin induced TREK-1 co-expression and annexin A2 secretion: role in trabecular meshwork cell elongation and motility. PLoS One. 2011; 6:e23070. [PubMed: 21886777]

[19]. Goel M, Sienkiewicz AE, Picciani R, Wang J, Lee RK, Bhattacharya SK. Cochlin, intraocular pressure regulation and mechanosensing. PLoS One. 2012; 7:e34309. [PubMed: 22496787]

[20]. Lee ES, Gabelt BT, Faralli JA, Peters DM, Brandt CR, Kaufman PL, Bhattacharya SK. COCH transgene expression in cultured human trabecular meshwork cells and its effect on outflow facility in monkey organ cultured anterior segments. Invest Ophthalmol Vis Sci. 2010; 51:2060–2066. [PubMed: 19933177]

[21]. Bhattacharya SK, Rockwood EJ, Smith SD, Bonilha VL, Crabb JS, Kuchtey RW, Robertson NG, Peachey NS, Morton CC, Crabb JW. Proteomics reveal Cochlin deposits associated with glaucomatous trabecular meshwork. J Biol Chem. 2005; 280:6080–6084. [PubMed: 15579465]

[22]. Chatterjee A, Villarreal G Jr. Oh DJ, Kang MH, Rhee DJ. AMP-activated protein kinase regulates intraocular pressure, extracellular matrix, and cytoskeleton in trabecular meshwork. Invest Ophthalmol Vis Sci. 2014; 55:3127–3139. [PubMed: 24713487]

[23]. Gomez-Cabrero A, Comes N, Gonzalez-Linares J, de Lapuente J, Borras M, Pales J, Gual A, Gasull X, Morales M. Use of transduction proteins to target trabecular meshwork cells: outflow modulation by profilin I. Mol Vis. 2005; 11:1071–1082. [PubMed: 16357826]

[24]. Syriani E, Cuesto G, Abad E, Pelaez T, Gual A, Pintor J, Morales M, Gasull X. Effects of platelet-derived growth factor on aqueous humor dynamics. Invest Ophthalmol Vis Sci. 2009; 50:3833–3839. [PubMed: 19357356]

[25]. Chen J, Runyan SA, Robinson MR. Novel ocular antihypertensive compounds in clinical trials. Clin Ophthalmol. 2011; 5:667–677. [PubMed: 21629573]

[26]. Tian B, Kaufman PL. Effects of the Rho kinase inhibitor Y-27632 and the phosphatase inhibitor calyculin A on outflow facility in monkeys. Exp Eye Res. 2005; 80:215–225. [PubMed: 15670800]

[27]. Lu Z, Overby DR, Scott PA, Freddo TF, Gong H. The mechanism of increasing outflow facility by rho-kinase inhibition with Y-27632 in bovine eyes. Exp Eye Res. 2008; 86:271–281. [PubMed: 18155193]

[28]. Ethier CR, Read AT, Chan DW. Effects of latrunculin-B on outflow facility and trabecular meshwork structure in human eyes. Invest Ophthalmol Vis Sci. 2006; 47:1991–1998. [PubMed: 16639007]

[29]. Peterson JA, Tian B, Bershadsky AD, Volberg T, Gangnon RE, Spector I, Geiger B, Kaufman PL. Latrunculin-A increases outflow facility in the monkey. Invest Ophthalmol Vis Sci. 1999; 40:931–941. [PubMed: 10102290]

[30]. Spector I, Shochet NR, Kashman Y, Groweiss A. Latrunculins: novel marine toxins that disrupt microfilament organization in cultured cells. Science. 1983; 219:493–495. [PubMed: 6681676]

[31]. Uehata M, Ishizaki T, Satoh H, Ono T, Kawahara T, Morishita T, Tamakawa H, Yamagami K, Inui J, Maekawa M, Narumiya S. Calcium sensitization of smooth muscle mediated by a Rho-associated protein kinase in hypertension. Nature. 1997; 389:990–994. [PubMed: 9353125]

[32]. McKee CT, Wood JA, Shah NM, Fischer ME, Reilly CM, Murphy CJ, Russell P. The effect of biophysical attributes of the ocular trabecular meshwork associated with glaucoma on the cell response to therapeutic agents. Biomaterials. 2011; 32:2417–2423. [PubMed: 21220171]

[33]. Morgan JT, Wood JA, Walker NJ, Raghunathan VK, Borjesson DL, Murphy CJ, Russell P. Human Trabecular Meshwork Cells Exhibit Several Characteristics of, but Are Distinct from, Adipose-Derived Mesenchymal Stem Cells. J Ocul Pharmacol Ther. 2014; 30:254–266. [PubMed: 24456002]

[34]. Mahaffy RE, Shih CK, MacKintosh FC, Kas J. Scanning probe-based frequency-dependent microrheology of polymer gels and biological cells. Phys Rev Lett. 2000; 85:880–883. [PubMed: 10991422]

[35]. Filla MS, Schwinn MK, Nosie AK, Clark RW, Peters DM. Dexamethasone-associated cross-linked actin network formation in human trabecular meshwork cells involves beta3 integrin signaling. Invest Ophthalmol Vis Sci. 2011; 52:2952–2959. [PubMed: 21273548]

[36]. Filla MS, Woods A, Kaufman PL, Peters DM. Beta1 and beta3 integrins cooperate to induce syndecan-4-containing cross-linked actin networks in human trabecular meshwork cells. Invest Ophthalmol Vis Sci. 2006; 47:1956–1967. [PubMed: 16639003]

[37]. Gordon WE 3rd, Bushnell A. Immunofluorescent and ultrastructural studies of polygonal microfilament networks in respreading non-muscle cells. Exp Cell Res. 1979; 120:335–348. [PubMed: 374104]

[38]. Lazarides E. Actin, alpha-actinin, and tropomyosin interaction in the structural organization of actin filaments in nonmuscle cells. J Cell Biol. 1976; 68:202–219. [PubMed: 1107334]

[39]. Gordon WE 3rd. Immunofluorescent and ultrastructural studies of “sarcomeric” units in stress fibers of cultured non-muscle cells. Exp Cell Res. 1978; 117:253–260. [PubMed: 363439]

[40]. Feramisco JR. Microinjection of fluorescently labeled alpha-actinin into living fibroblasts. Proc Natl Acad Sci U S A. 1979; 76:3967–3971. [PubMed: 291056]

[41]. Feramisco JR, Blose SH. Distribution of fluorescently labeled alpha-actinin in living and fixed fibroblasts. J Cell Biol. 1980; 86:608–615. [PubMed: 7190570]

[42]. Clark AF, Miggans ST, Wilson K, Browder S, McCartney MD. Cytoskeletal changes in cultured human glaucoma trabecular meshwork cells. Journal of glaucoma. 1995; 4:183–188. [PubMed: 19920666]

[43]. Clark AF, Wilson K, McCartney MD, Miggans ST, Kunkle M, Howe W. Glucocorticoid-induced formation of cross-linked actin networks in cultured human trabecular meshwork cells. Invest Ophthalmol Vis Sci. 1994; 35:281–294. [PubMed: 8300356]

[44]. Filla MS, Schwinn MK, Sheibani N, Kaufman PL, Peters DM. Regulation of cross-linked actin network (CLAN) formation in human trabecular meshwork (HTM) cells by convergence of distinct beta1 and beta3 integrin pathways. Invest Ophthalmol Vis Sci. 2009; 50:5723–5731. [PubMed: 19643963]

[45]. Hoare MJ, Grierson I, Brotchie D, Pollock N, Cracknell K, Clark AF. Cross-linked actin networks (CLANs) in the trabecular meshwork of the normal and glaucomatous human eye in situ. Invest Ophthalmol Vis Sci. 2009; 50:1255–1263. [PubMed: 18952927]

[46]. Lazarides E, Burridge K. Alpha-actinin: immunofluorescent localization of a muscle structural protein in nonmuscle cells. Cell. 1975; 6:289–298. [PubMed: 802682]

[47]. Lin ZX, Holtzer S, Schultheiss T, Murray J, Masaki T, Fischman DA, Holtzer H. Polygons and adhesion plaques and the disassembly and assembly of myofibrils in cardiac myocytes. J Cell Biol. 1989; 108:2355–2367. [PubMed: 2472405]

- Lat B treated trabecular meshwork cells form cortical actin arrays after washout.
- Peak array formation correlates with previous study showing increased stiffness.
- ROCK inhibition via Y-27632 results in neither array formation nor stiffening.

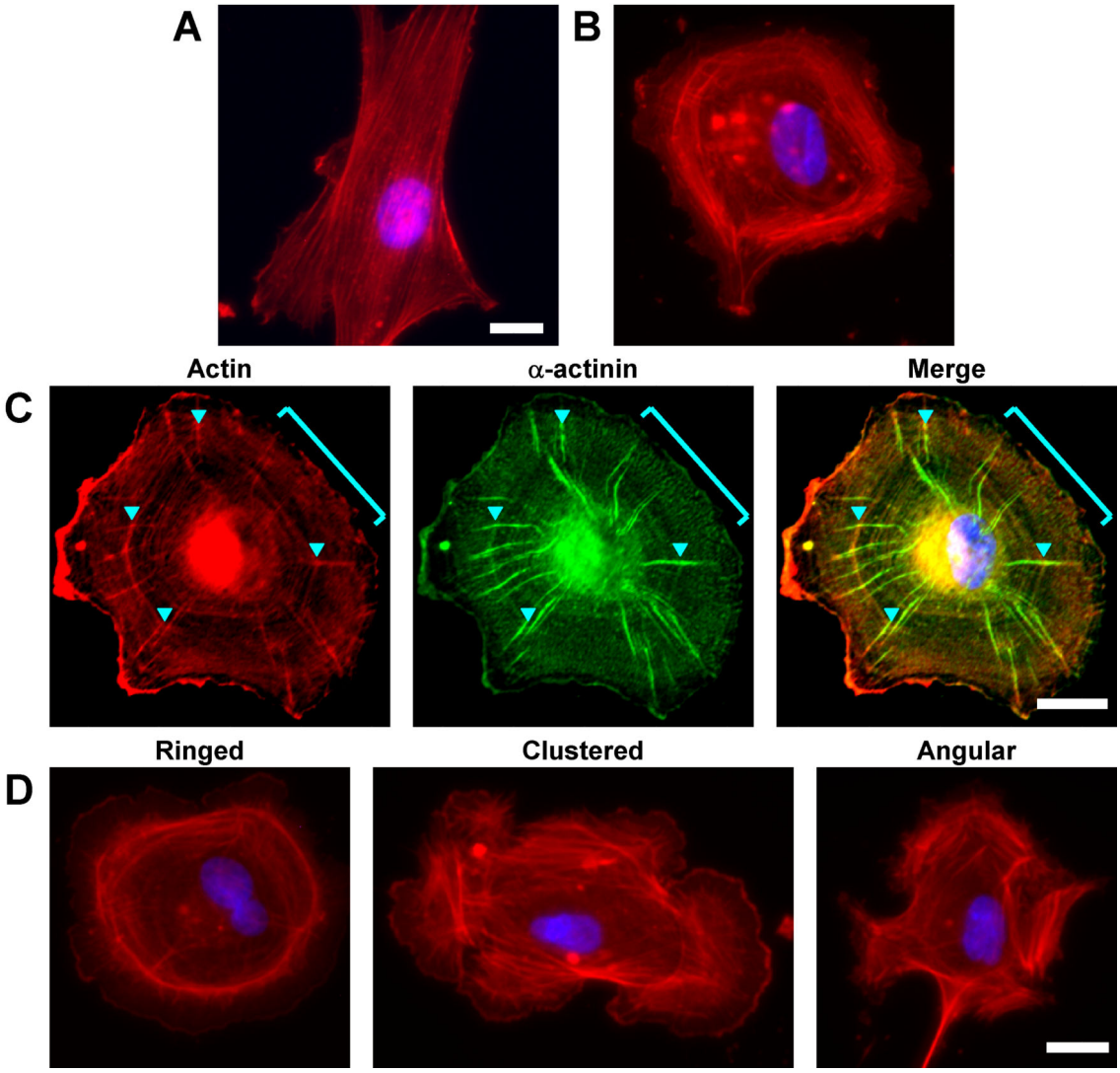

Figure 1.

Demonstration of CAA formation in HTM cells. (A) Phalloidin stain of a typical HTM cell in culture, displaying prominent axial stress fibers with. (B) Cortical actin array in an isolated HTM cell stained with phalloidin. (C) Representative image of α-actinin labeling of both the radial and cortical actin structures with enrichment at the junctions (arrowheads). Periodic α-actinin labeling of circumferential actin (bracketed region) was also observed. (D) Three major phenotypes of CAAs. All nuclei are labeled with DAPI (blue). All scale bars are 20 μm.

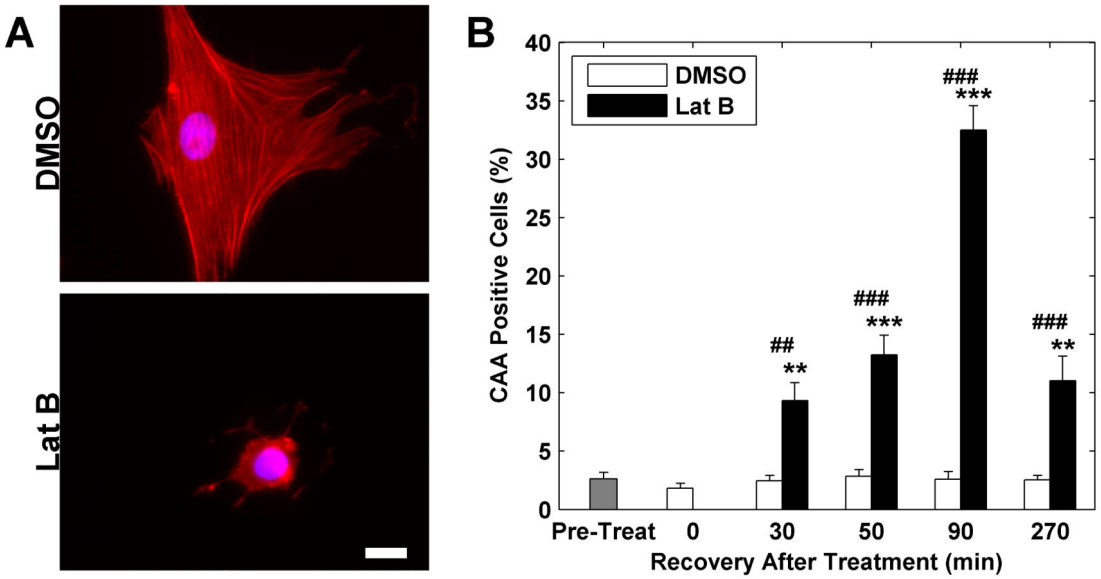

Figure 2.

Induction of CAAs via Lat B treatment. (A) Phalloidin staining of control (DMSO) and Lat B treated cells at 30 min. The application of 2 μM Lat B completely removed phalloidin staining of stress fibers typical of control cells. (B) HTM cells exhibited CAAs during recovery from Lat B, but not control (DMSO) treatments. Phalloidin staining is shown in red; nuclei are labeled with DAPI (blue). Scale bar is 20 μm.

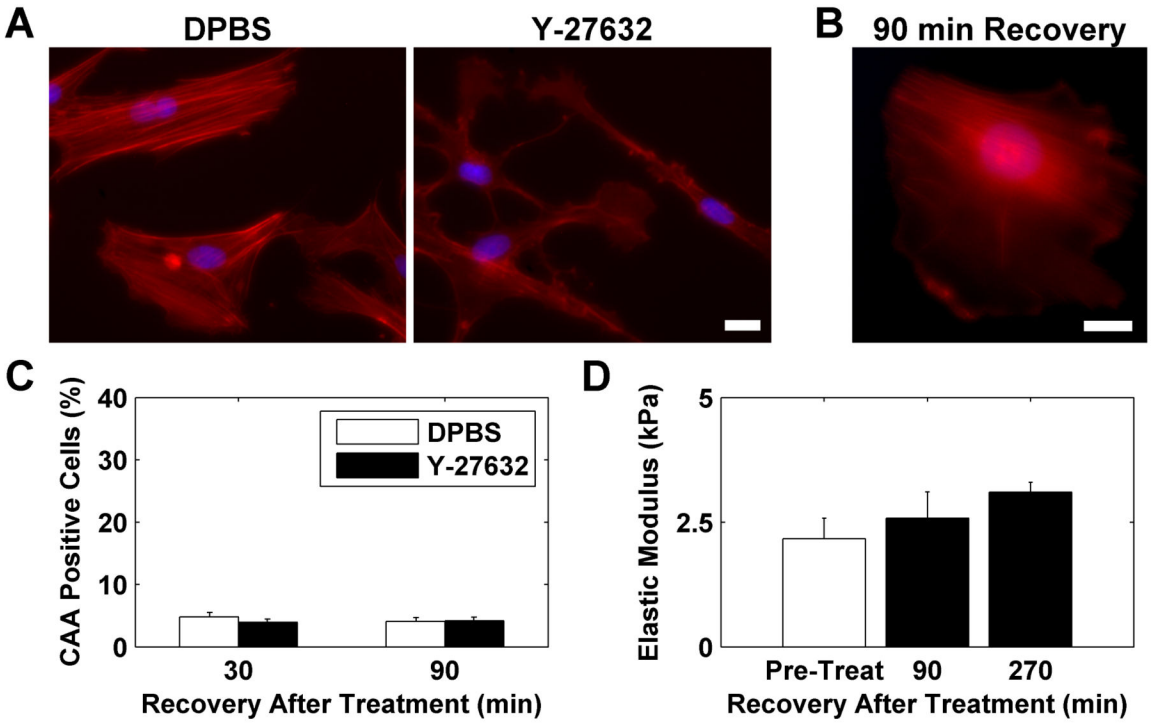

Figure 3.

Y-27632 had minimal impact on CAA formation or cell mechanics. (A) Phalloidin staining (red) of control (DPBS) and Y-27632 treated cells at 30 min. 100 μM Y-27632 was sufficient to completely inhibit stress fibers typical of control cells (B) After 90 minutes of recovery, Y-27632 treated cells still had altered morphology, although uniaxial stress fibers had begun to appear. (C) Y-27632 treatment did not induce CAA formation during recovery. (D) Y-27632 treatment did not alter cellular mechanics during recovery. Phalloidin staining is shown in red; nuclei are labeled with DAPI (blue). Scale bars are 20 μm.

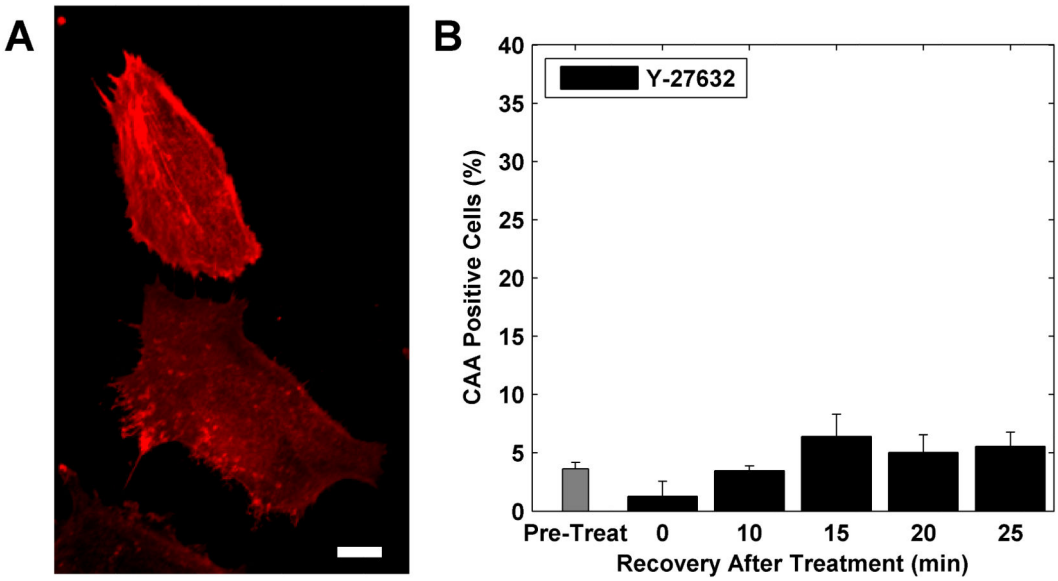

Figure 4.

Y-27632 had minimal impact on CAA formation at earlier timepoints. (A) Phalloidin staining of HTM cells 15 minutes after Y-27632 washout. The actin cytoskeleton is largely disrupted but visible filaments are forming in some cells. Scale bar is 20 μm. (B) Y-27632 treatment did not induce CAA formation at earlier timepoints during recovery.